Journal of Applied Polymer Science

Recovery and characterization of lignin from alkaline straw pulping black liquor: As feedstock for bio-oil research

Zhengbin Tian, Lei Zong, Rujie Niu, Xiao Wang, Yan Li, Shiyun Ai
College of Chemistry and Material Science, Shandong Agricultural University, 271018, Taian, Shandong, People's Republic of China
Correspondence to: Y. Li (E-mail: liyan2010@sdau.edu.cn) and S. Ai (E-mail: ashy@sdau.edu.cn)

ABSTRACT: Conversion of lignin derived from lignocellulosic biomass to bio-oil has the promising potential to significantly reduce petroleum dependence. For that purpose, it is necessary to search for a low-cost lignin source. In this study, lignin sample was separated from straw pulping black liquor by HCl-precipitation, followed by extraction with a mixture of dioxane and water. The content of lignin in the total black liquor solid reached up to 34.8%, determined by UV spectroscopy, and the yield could account for 74.4% of the total lignin composition. The structure of lignin was investigated by various spectroscopic techniques such as FTIR, ^{1}H-NMR, XRD, and XPS. The structural analysis revealed that recovered lignin preserved basic lignin structure, but had relatively lower amount of β-O-4 linkages. The molecular weights were studied through THF-eluted GPC showing that separated lignin had the low M_n, which was favorable for the full degradation process during conversion of lignin to bio-oil. Therefore, a feasible solution for effective utilization of lignin in straw pulping black liquor as feedstock for bio-oil was proposed in the study. © 2015 Wiley Periodicals, Inc. J. Appl. Polym. Sci. **2015**, *132*, 42057.

KEYWORDS: cellulose and other wood products; degradation; oil and gas

Received 24 September 2014; accepted 28 January 2015
DOI: 10.1002/app.42057

INTRODUCTION

Bio-oils, sustainably produced from abundant lignocellulosic biomass, have attracted global attention as a promising alternative for fossil production to reduce petroleum dependence.[1,2] Lignin is a natural randomized alkyl-aromatic based biopolymer that can comprise up to 15–30% (by weight) of the lignocellulosic biomass, depending on the nature of the biomass.[3] It is an amorphous material with a complex three-dimensional structure arising from its enzymatic polymerization of phenoxypropyl monomers, including p-coumaryl alcohol, coniferyl alcohol, and sinapyl alcohol.[4] The phenyl propane units are linked by several different types of linkages, including β-O-4, 5-5′, β-5, 4-O-5, and β-1, among which C—O—C ether linkages account for 67–75%.[3,5] As lignin includes high-value aromatic compounds (phenols), it may become a possible raw feedstock for bio-oil by the ether cleavage. However, it is difficult to separate lignin from biomass, due to the insolubility and complex nature (interactions with cellulose, hemicellulose, and other cell wall matrix components). Physical, chemical, or biological pretreatments are used to detach lignin from biomass, which obviously presents a major challenge in the bio-oil production at commercial level due to the high cost.[6] Therefore, one important step in the conversion of lignocellulosic biomass to bio-oil is to find economical source of lignin.

Black liquor is highly viscous aqueous waste considered as one of the primary by-products of the pulping industry. It is generally known that black liquor is a kind of toxic and severely colored paper pulping sewage, consisting of inorganic pulping chemicals and organics from extracted biomass constituents. The solid content of black liquor varies between 15% and 40% by weight, whereas lignin accounts for 30–45% of the total solid composition.[7] Paper pulp can be mainly divided into wood pulp and straw pulp due to raw material. In wood alkaline pulping the black liquor processing technology is quite mature, including chemical regeneration by utilizing lignin as an energy source for burning in soda recovery boiler. However, straw is generally used as raw material for paper pulp due to the shortage of wood resources in China. Black liquor of straw pulp contains a large amount of silica and fiber fines, which is not favorable for alkali recovery. Therefore, separation and use of lignin in straw pulping black liquor becomes an alternative way of reusing black liquor instead of alkali recovery. Although million tons of lignin is produced in black liquor annually, only a small amount was used as precursor for the preparation of activated carbon.[8] The left is

Additional Supporting Information may be found in the online version of this article.

burned even poured into the rivers, resulting in resources waste as well as water pollution. The discharge of black liquor to river would significantly increase the biological oxygen demand (BOD) and chemical oxygen demand (COD) in aquatic environments, which are responsible for serious damage to the water body and human health.[7] So, if the waste lignin in black liquor is utilized for example as a feedstock for bio-oil production, a significant opportunity would be generated for enhancing the economic viability, carbon conversion rate, overall operational efficiency, and sustainability of befouls and chemical production, in conformity with the requirements of sustainable development and resource-conserving economy.[2] Thus it is very important to separate and characterize lignin from straw pulping black liquor.

Lignin can be separated by various methods, among of which, dissolution in alkali and acid precipitation is considered to be the most common method to isolate lignin from biomass materials. It is known that lignin undergoes solubilization and aggregation process with increase and decrease of pH due to the deprotonation and protonation of ionizable groups in lignin. This phenomenon can be exploited for crude lignin recovery from alkaline black liquors, in which the pH is decreased with an acidifying reagent such as CO_2, acetic acid, or H_2SO_4.[9] The resultant lignin precipitate is usually recovered by centrifugation instead of filtration, due to its high viscosity.

Various spectroscopic methods have been applied to illustrate the lignin structure qualitatively and quantitatively. UV/Vis spectroscopy is one of the most friendly and adaptable analytical techniques and has already been reported to quantify the concentration of lignin in black liquor generated from different biomass. Usually, the quantitative determination of lignin concentration is dependent on two characteristic adsorptions at 200–230 and 260–280 nm, respectively.[10] FTIR (Fourier Transform Infrared Spectroscopy) and ^{1}H-NMR (Nuclear Magnetic Resonance) are used to analyze the functional groups qualitatively and semiquantitatively. XPS (X-ray photoelectron spectroscopy) has been applied increasingly to the surface characterization of lignocellulosic materials and now focuses attention on the surface components.

In this work, lignin sample was separated from alkaline straw pulping black liquor by HCl-precipitation, followed by extraction with a mixture of dioxane and water, to remove impurities like fatty acids and polysaccharides. The content of lignin in black liquor was determined by UV spectroscopy through the calibration curve equation. To research the possibility of conversion of separated lignin to bio-oil, the structure of lignin was investigated by various spectroscopic techniques such as FTIR, ^{1}H-NMR, XRD (X-ray diffraction), and XPS. The molecular weights of the lignin preparations were evaluated by GPC (gel permeation chromatography) and the thermal behavior was examined by TGA (thermogravimetric analysis). The morphology and size of lignin was observed by SEM (scanning electron microscope).

EXPERIMENTAL

Materials

The feedstock powder containing alkali lignin dried directly from straw pulping black liquor was supplied by the Quanlin paper mill in Shandong province, China. HPLC grade tetrahydrofuran (THF) was purchased from Aladdin. Commercial lignin (CML, 98%) was purchased from Shengfujiang Chemical (Tianjin, China). Other chemicals were analytical grade and not further purified prior to using. Dioxane, pyridine, acetic anhydride, and Concentrated HCl (12 mol/L) were purchased from Aladdin. Ethanol was purchased from Yongda Chemical Reagent (Tianjin, China). Distilled deionized water was utilized through the experiments.

Separation and Purification of Lignin

Generally, alkali lignin could be precipitated through acidification and higher temperature contributes to better precipitated lignin solubility.[11] Therefore, lignin can be separated from pulping black liquor and purified through this process. Briefly, the powder was dispersed in deionized water, centrifuged to separate insoluble substance and acidified to the pH of 1 with concentrated HCl at a certain temperature. After aging for a period of time, crude lignin precipitate was separated by centrifugation and washed several times. Crude lignin was purified in Soxhlet extractor with a solution dioxane and water (9 : 1, v/v). After refluxing for 2 h, the dark clear solution was centrifuged and subsequently poured into ice water (pH = 2.0, measured with an acidometer) to induce precipitation. The precipitate was centrifuged and washed with ethanol for two times, followed with deionized water for three times. Purified lignin (PFL) was obtained after centrifugation and freeze-drying (described in Figure S2, Supporting Information).

The Acetylation of Lignin

PFL sample was acetylated to improve its dissolvability in the solvents for GPC and ^{1}H NMR analysis according to a literature method with some modifications.[12] One gram of lignin was dissolved in 40 mL of a mixture of purified pyridine and acetic anhydride (1 : 1, v/v). After stirring for 24 h at room temperature under the exclusion of sunlight, the mixture was concentrated under reduced pressure by adding ethanol for several times. The mixture was dropped slowly into 200 mL of ice water (pH = 2.0) to induce precipitation, and the precipitate was washed with deionized water (3 × 50 mL). After centrifugation and freeze-drying, acetylated lignin was produced.

UV Quantification

Reference solutions of CML dissolved in 0.01*M* NaOH were obtained with the concentration of 0.01, 0.02, 0.03, 0.04, 0.05, and 0.06 g/L. UV spectroscopy between 190 and 400 nm of varied lignin fractions were recorded using a Shimadzu Vis-spectrometer (UV-2450, Japan) in double-beam mode using an uncovered and cleaned quartz cell. UV spectra of feedstock and PFL with the concentration of 0.1015 and 0.0413 g/L, respectively, were also recorded.

Characterizations

The surface functional groups in lignin were measured by FTIR using Thermo Scientific Nicolet 380 Spectrometer, USA. The samples were dispersed in a matrix of KBr (1 : 100), followed by an appropriate compression to form pellets. For each sample, the spectrum was investigated in absorbance units with a spectral range from 4000 to 400 cm^{-1} at a spectral resolution of

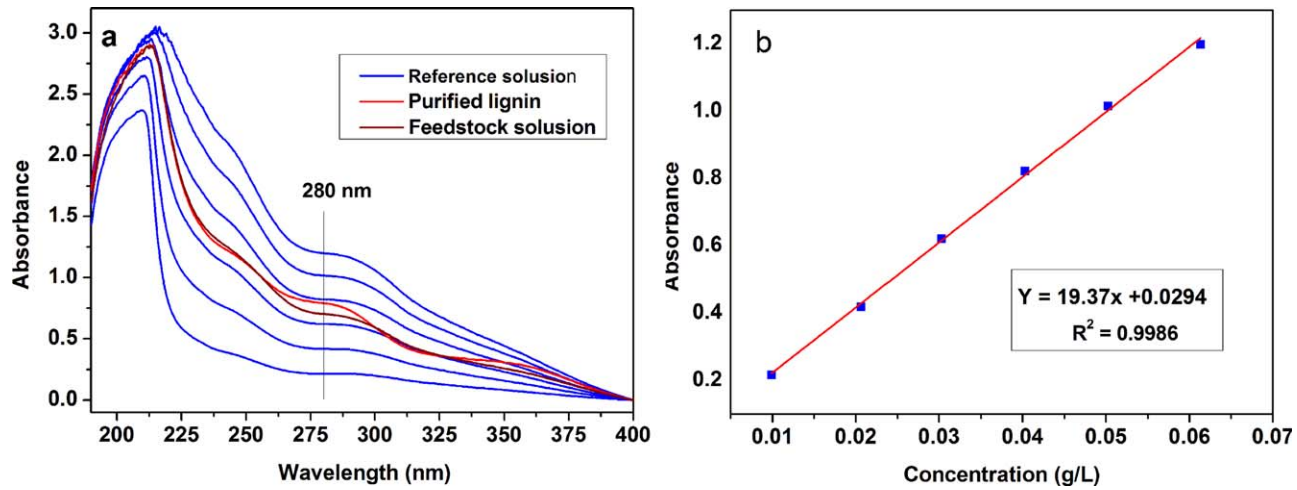

Figure 1. (a) Shows the UV spectra for lignin at various concentrations and (b) shows the graph of lignin concentration against absorbance at 280 nm, proving a linear relationship obeying the Beer–Lambert Law. [Color figure can be viewed in the online issue, which is available at wileyonlinelibrary.com.]

4 cm^{-1} and 32 scans. The background (measured in air) was subtracted from the FTIR spectra.

The ^1H NMR spectra of 50 mg acetylated lignin solved in 1.0 mL dimethyl-d6 sulfoxide (DMSO-d6) were recorded at room temperature, using tetramethylsilane (TMS) as the internal standard in a Bruker Avance 300 spectrometer (Bruker, Germany) with an operating frequency at 300 MHz.

XRD patterns were measured at room temperature by using a Bruker D8 Advance X-ray diffractometer with the Cu Kα radiation at 40 kV and 30 mA. The data was collected in a 2θ range from 5° to 80° with a scanning speed of 2°min^{-1}.

XPS was measured with a K-Alpha XPS system (Thermo Fisher Scientific, USA) using a monochromatic Al Kα as the excitation source. Survey (wide) scans spanned from 1100 to 0 eV binding energy, which were collected with an analyzer pass energy of 100 eV at an interval of 1.00 eV. Multiplex (narrow) high-resolution spectra of the C1s region from 281 to 291 eV and the O1s region from 528 to 537 eV were collected respectively with an analyzer pass energy of 30 eV at an interval of 0.05 eV.

Thermal analysis of lignin was performed using thermogravimetric analysis (TGA) on a simultaneous thermal analyzer (SDT Q600, TA, USA) from room temperature to 800°C. Amounts of about 10 mg sample were heated in an aluminum crucible with a heating rate of 10°C/min in a nitrogen atmosphere flow of 30 mL/min.

GPC analyses were performed to measure the weight average (M_w) and number-average (M_n) molecular weights on an UltiMate3000 apparatus (Dionex, USA) using a UV spectrophotometer at 280 nm. The mobile phase was THF and ran at a flow rate of 1 mL/min. Relative average molecular weights were determined using calibration with polystyrene standards ($K = 0.011$ mL/g, $\alpha = 0.735$).

SEM analysis was carried out using a NoVa™ Nano SEM 430 scanning electron microscope (FEI, USA) at an electron acceleration voltage of 20 kV. Prior to scanning, the samples were coated with a thin layer of gold using a sputter coater to make them conductive.

RESULTS AND DISCUSSION

UV Analysis and Lignin Quantification

UV spectroscopy of CML dissolved in 0.01 mol/L NaOH solution at 190–400 nm was studied. As shown in Figure 1(a), an apparent regularity to the variation in the UV peak height appears with little or no change in the shape of the spectra, as the isolated lignin fractions changes. The maximum absorption appears around 210 nm and a shoulder appears near 280 nm, which was associated with nonconjugated phenolic groups (aromatic rings) of lignin.[13] It has been detected that the guaiacyl structures show maximum absorption in the 280 nm and the syringyl monomer absorbs less light at the same region.[14] The weak absorption at 350 nm was ascribed to conjugated phenolic groups such as ferulic and p-coumaric acids.[15] The UV response of lignin at 280 nm (traditionally utilized wavelength to lignin concentration determination) can be hardly affected by polysaccharides and their derived production only at low concentration.[10] Therefore, adsorptions were obtained at 280 nm used for calibration curves and concentration determination in this study, as shown in Figure 1(b). It can be seen that there is a significant liner correlation between the adsorption and lignin concentrations ranging from 0.01 to 0.06 g/L in 0.01 mol/L NaOH solution. The extinction coefficient value (ε, L g^{-1} cm^{-1}) calculated using the Beer-Lambert equation was 19.37. Content of lignin in raw material and purity of PFL could be obtained through the calibration curve equation. Eventually, the content of lignin was 34.8% and purity of PFL could reach to 95.2% by calculation.

The lignin yield was calculated with the following equation:

Lignin yield (%) = (Mass of lignin product/Mass of lignin in raw material) × 100

Effects of different conditions on the lignin yield were discussed. From the data (Table I), it can be seen that lignin yield showed

Table I. Effects of Different Conditions on the Lignin Yield

Label	pH	Acidification temperature (°C)	Ageing time (min)	Lignin yield (%)
1	1.0	20	30	74.3
2	1.0	40	30	73.9
3	1.0	60	30	74.4
4	1.0	20	60	74.1
5	1.0	20	90	74.4
6	2.0	20	30	60.3
7	3.0	20	30	20.7
8	4.0	20	30	5.93

no significant differences among the acidification temperature of 20–60°C and ageing time of 30–90 min. However, the high temperature resulted in aggregation of lignin, which eased the separation in the centrifugation process. According to the data, it was clearly that the lignin yield decreased sharply when pH increased from 1 to 4, which may be attributed to the incomplete precipitation of alkali lignin in weak acidic condition. Furthermore, lignin redispersed in water with pH increasing after washing for several times. The low pH is needed for hindering lignin dispersing in water.

The results of lignin separated by other methods and from different material were tabulated in Table II. Milling is an excellent method to obtain lignin with similar chemical structure in biomass; however, it usually obtained a low yield. A pretreatment process like steam explosion was needed to gain a high yield. Solvent extraction under high temperature was also frequently applied in lignin extraction from biomass materials. The yield was drastically influenced by various factors, such as solvent, extraction time, and temperature. Generally, higher temperature and longer time contributes to better extractability in solvent extraction method, which was difficult to apply into large-scale production due to the high cost. Alkali-solution and acid-isolation method was considered to be the most common method to obtain lignin from biomass materials. Meanwhile, a high yield can be achieved easily. In the work, the raw material, straw pulping black liquor, containing abundant alkali lignin

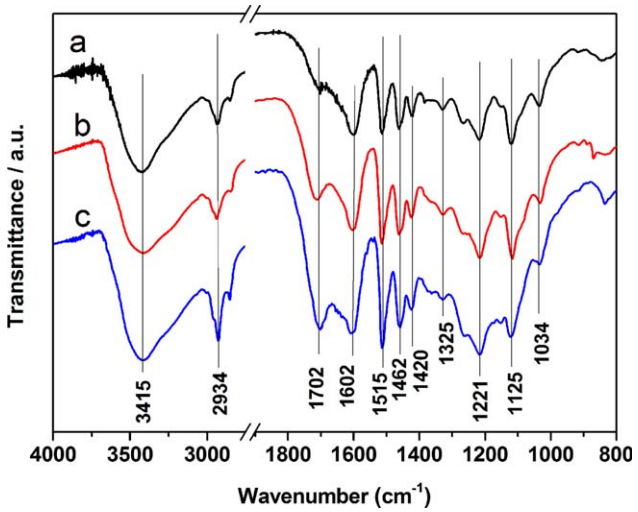

Figure 2. FTIR spectra of lignin: (a) PFL, (b) crude lignin, and (c) CML. [Color figure can be viewed in the online issue, which is available at wileyonlinelibrary.com.]

was equivalent to the production through an alkali-solution process and lignin can be directly precipitated by adding acid. It is an easy and economic method, which also offered a proposal to solve the problem of effective utilization of pulping black liquor.

FTIR and ^{1}H-NMR Analysis

The spectra of FTIR analysis involved most of lignin's characteristic functional groups. Figure 2 shows the FTIR spectra of the crude lignin, PFL, and CML. The peak positions of the major absorption bands assigned the corresponding functional groups are summarized in Table III according to the Refs. [16,17]. In general, the positions of the peaks in all three spectra are globally rather similar, except for a minor shifting of some peaks. The broad band at around 3100–3700 cm^{-1} was due to hydroxyl groups, indicating that a large number of hydroxyl groups existed in the separated lignin, and some of which may have been derived from the breakage of β—O—4 ether bonds in pulping process. The carbonyl group appeared in the range between 1715 and 1700 cm^{-1}, not in 1675–1660 cm^{-1},

Table II. Comparison of Lignin Separated by Other Methods

Raw material	Method	Solvent	Yield (%)	Ref.
Bio-ethanol production residue	Solvent extraction	Benzyl alcohol	71.55	11
	Alkali-acid isolation	NaOH	65.05	
Bamboo	Ball-milling	-	19.56	12
	Solvent extraction	DMSO/NMI	26.08	
	Alkali-solution	NaOH	66.52	
Eucalyptus	Solvent extraction	Ionic liquid/toluene	15.4	30
		Alkaline ethanol	23.3	
Wheat straw	Ball-milling	-	ca. 20	31
Steam-exploded eucalyptus	Phase separation/milling	-	75.0	32

Table III. FTIR Peak Positions and Assignments of Lignin

Wave number (cm^{-1})	Band origin
3415	O—H stretching vibration in aromatic and aliphatic OH groups
2934, 2845	C—H stretching vibration in the methyl and methylene groups
1702	Unconjugated carbonyl/carboxyl stretch
1602	Aromatic ring vibrations of the phenylpropane groups
1515	Aromatic ring vibrations of the phenylpropane groups plus C—C bounds
1462	Aromatic ring vibration
1420	C—H in-plane deformation with aromatic structure vibrations
1383	Aliphatic C—H and O—H stretch
1325	Syringyl ring breathing with C—O stretching vibration
1267	Guaiacyl ring breathing with C—O stretching vibration
1221	C—O stretching vibration of phenolic hydroxyl and phenolic ether
1150	Aromatic C—H in-plane deformation in the guaiacyl ring
1121	Aromatic C—H in-plane deformation in the syringyl ring
1034	Aromatic C—H in-plane deformation plus C—O deformation in primary alcohols plus C=O stretch (unconjugated)
845	C—H out-of-plane deformation vibration

indicating that C=O bond is in nonconjugation with the aromatic rings.[18] Obviously, the peak at 1702 cm^{-1} of PFL was much weaker than that of CML, which may be attributed to the partly breakage of C—O bond in pulping process. The peaks at 1602, 1515, and 1462 cm^{-1} were assigned to the aromatic skeletal vibration, which is a fundamental structure of lignin. The typical C—H band in acetate methyl group was observed at 1383 cm^{-1}, which suggested that natural acetylation exists in the obtained lignin. Typical grass lignin patterns were exhibited in the fingerprint regions of the FTIR spectra of the lignin preparations, with a dominating peak at 1125 cm^{-1} as an unmistakable signal of a guaiacyl-syringyl (GS) lignin.[12] The spectra of crude lignin at 1000–1300 cm^{-1} was not fine and much more intense than that of PFL, as C—H deformation in carbohydrates has absorption in the same region. This suggested existence of some impurity in crude lignin and it was necessary for further purification. However, a small amount of carbon was detected by XRD (Figure 1S, Supporting Information) in PFL, proving that a carbonization reaction occurred in the purge process. Moreover, a broad embossment appeared in the pattern with the absence of any sharp diffraction of cellulose etc., indicating that lignin had an amorphous characteristic.

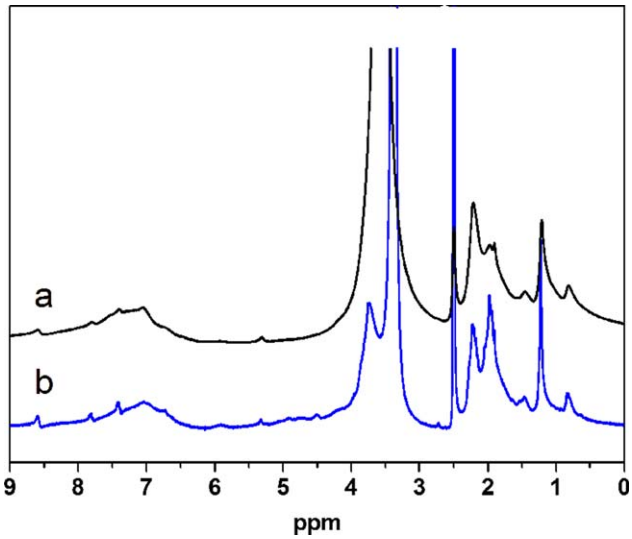

Figure 3. ^{1}H NMR spectra of (a) acetylated CML and (b) acetylated PFL. [Color figure can be viewed in the online issue, which is available at wileyonlinelibrary.com.]

The chemical structure of lignin sample can also be investigated through ^{1}H NMR spectra. Figure 3 shows the ^{1}H NMR spectra of acetylated PFL and CML samples, and Table IV lists the position of signals assigned.[19,20] H_2O and DMSO-d6 aroused the two signals at δ_H 2.5 and 3.3 ppm, respectively. All the signals between 6.5 and 8.0 ppm can be attributed to aromatic protons in S and G units. In the CML spectra, the signals around 3.3 ppm were covered by the signal DMSO-d6. In the PFL spectra, the β—O—4 ether bond, the most common coupling linkage between lignin units, showed only a weak resonance at 4.7 ppm. This suggested that separated lignin from black liquor had undergone some degree of degradation, which was consistent with the FTIR results. Unsurprisingly, the relative content of the hydroxyl group signals from 1.7 to 2.4 ppm was high, because some of them were released by the breakage of ether linkages during the degradation of the lignin. Methoxyl protons (—OCH_3), closely related to G/S proportion, had a strong resonance at 3.7 ppm.

Table IV. Peak Assignments for ^{1}H NMR Spectra

Range (ppm)	Assignment
8.6	H in carboxyl
8-6.5	Aromatic H
7.4-6.8	Aromatic H in G units
6.8-6.5	Aromatic H in S units
6.2-5.7	H_α of β-O-4 and β-1 structures
5.6-5.2	H_α in β-5 structures
4.3-4.9	H_α and H_β of β-O-4 structures
4.0-3.5	H in methoxyl group
2.7	H_β in β-β structures
2.1-2.4	H in aromatic acetates
1.7-2.1	H in aliphatic acetates
1.6-0.7	H in methylene and methyl

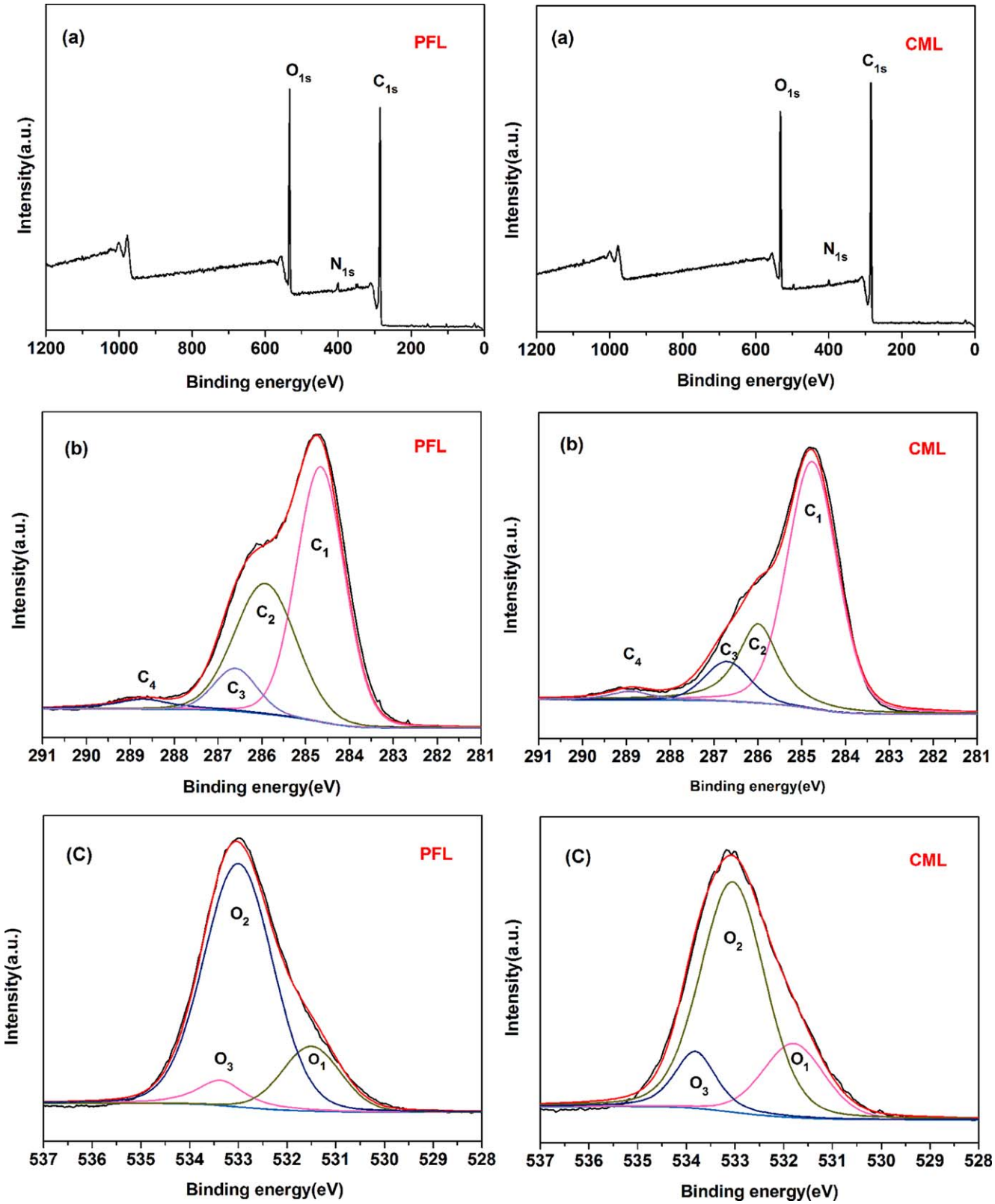

Figure 4. (a) A typical XPS wide scan (0–1200 eV) spectrum of lignin, (b) High resolution XPS spectra of C_{1s}, and (c) High resolution XPS spectra of O_{1s}. [Color figure can be viewed in the online issue, which is available at wileyonlinelibrary.com.]

Table V. XPS Binding Energies and Percent of Assigned Carbon Species

C type	Assignment	Binding energy (eV)		Percent of total carbon (%)	
		PFL	CML	PFL	CML
C_1	Adventitious carbon, hydrocarbon	284.8	284.7	53.5	66.2
C_2	Alcohols, esters, amines	285.9	286.0	35.1	21.9
C_3	Carbonyl, aldehydeketone	286.7	286.7	8.0	9.5
C_4	Carbon adjacent to carboxyl	288.6	288.9	3.3	2.4

Table VI. XPS Binding Energies and Percent of Oxygen Species

O type	Assignment	Binding energy (eV)		Percent of total carbon (%)	
		PFL	CML	PFL	CML
O_1	Carbonyl, esters, aldehydeketone	531.5	531.8	16.3	20.6
O_2	Alcohols, esters	532.9	533.1	75.2	67.3
O_3	Esters, phenol	533.7	533.9	8.5	12.1

It is difficult to acquire an accurate quantitative calculation for the peak integration of the functional group in the ^{1}H NMR spectra, as the peaks of lignin functional groups in the spectra overlap, due to the polymeric structure of lignin. However, the estimation of the ratio of aromatic/methoxyl groups and the ratio of aromatic/phenolic acetate could be made assuming that the aromatic proton signals around 7 are corresponding to the 2.5 H/aromatic ring for acetylated lignin and using the resonance of methoxyl protons as an internal standard.[21] Also, the following parameters can be calculated by integration: the ratio of S and G structures (S/G), the ratio of phenolic OH groups and aliphatic OH groups (OH_{ph}/OH_{al}) methoxyl groups and total hydroxyl groups per average phenylpropane unit (C9). The S/G ratio was estimated from the integration of aromatic protons and methoxyl groups and the OH_{Ph}/OH_{Al} ratio was calculated based on integration of aromatic and aliphatic acetates.[11]

XPS Analysis

XPS analysis is a practical surface analysis method, through which chemical and structural information on the material surface can be obtained. Also, XPS is very sensitive to the state of sample, and can be used to analyze all elements except hydrogen and helium. Therefore, to obtain information about the chemical environment and atomic concentrations presented in lignin, XPS analysis was performed. Figure 4(a) showed a typical XPS survey spectrum of PFL and CML, respectively. The results obviously revealed that carbon and oxygen were the major elements, which were demonstrated by the peak of C_{1s} at 284 eV and the peak of O_{1s} at 533 eV, and a small amount of nitrogen existed in lignin, which was demonstrated by the characteristic peak of N_{1s} at 400 eV. The relative distribution of the composition of carbon and oxygen atoms was determined by dividing the total integration area with the respective peak area. Then, the oxygen to carbon (O/C) ratio was obtained easily. The O/C ratio of PFL was 0.38, which was much higher than the value (0.27) of CML, which may be attributed to the oxidation and hydrolysis of PFL in the pulping.

High-resolution XPS scan was employed to further investigate the chemical valences of the surface elements. The carbon spectrum was resolved into the four main types of carbon atoms, [Figure 4(b)], namely:

C_1: C bound singly to other C and/or H;

C_2: C bound to a single noncarbonyl O or N;

C_3: C bound doubly to one carbonyl O or two noncarbonyl O;

C_4: C linked to one carbonyl O and one noncarbonyl O such as in a carboxylic acid or an ester.[22]

High resolution oxygen spectra were difficult to resolve. In this work, the oxygen spectrum was resolved into the three main

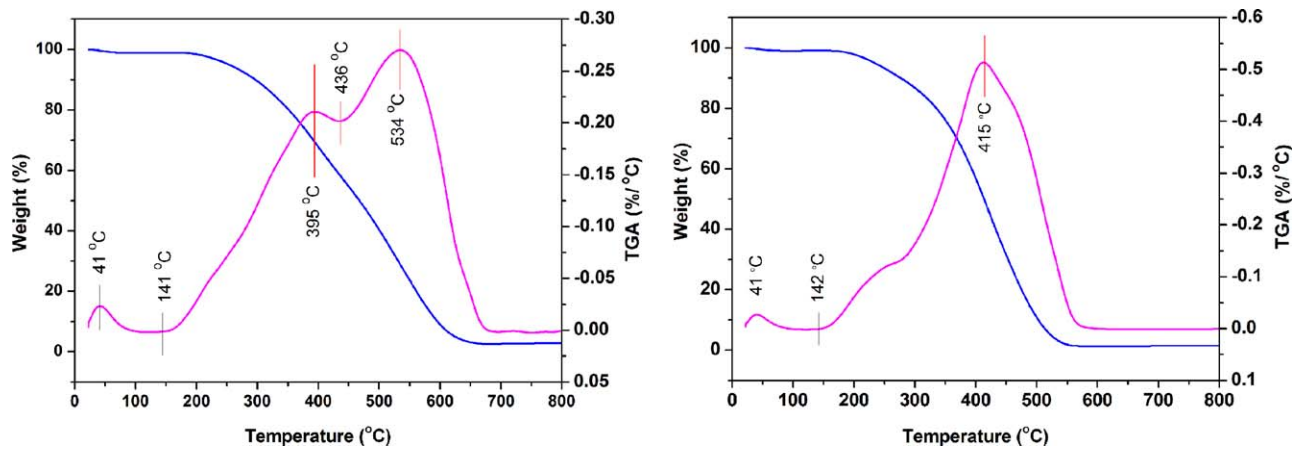

Figure 5. TG–DTG curves of (a) PFL and (b) CML under N_2. [Color figure can be viewed in the online issue, which is available at wileyonlinelibrary.com.]

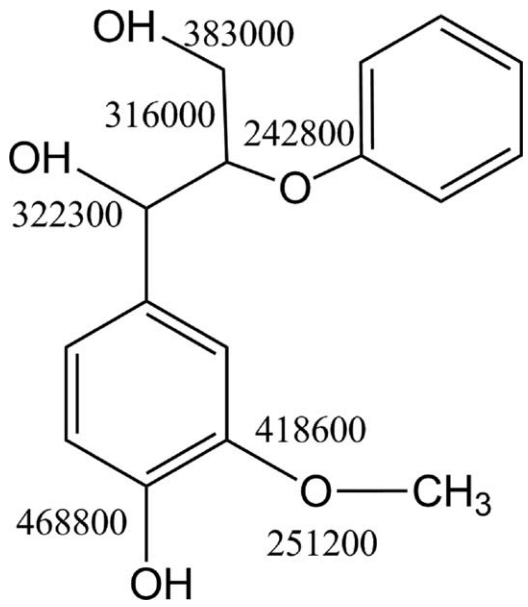

Figure 6. Typical bond energy [J/mol] in lignin structure.[24]

bands, each of which contained several possible bonds each with slightly different bonding energies, leading to broadening of the peaks. The bands have been labeled as O_1 at 531.6 eV; O_2 at 533.0 eV; and O_3 at 533.7 eV [Figure 4(c)]. The possible composition of each band was listed as follows:

O_1: C═O (aromatic) at 531.25 eV; C═O*—O (Aromatic) at 531.65 eV; C═O*—O (aliphatic) at 532.21 eV; C═O (aliphatic) at 532.33 eV

O_2: C—O—C at 532.6 eV; C—OH (aliphatic) at 532.9 eV; C═O—O*(aromatic) at 533.14 eV

O_3: C═O—O* (aliphatic) at 533.59 eV; aromatic OH at 533.64 eV.[23]

The element contents (percent of atomic type) for C and O are tabulated in Tables V and VI, respectively. C_1 and C_2 components were major constituents of C1s in lignin, while O_2 component was the main type in O_2. This suggested that hat oxygen was presenting mainly in lignin C—O bonds.

TGA Analysis

The research for thermal property of lignin is an important property for its applications in thermo-chemical conversion into bio-oil. The potential relationship between products and thermolysis temperature can be investigated by TG-FTIR or TG-MS technology. It is possible to forecast the appropriate temperature for destination product, once the relationship is established.

In the work, the thermal property of lignin was examined by TGA. TGA curves (Figure 5) revealed the relationship between the weight losses of lignin and temperature and the corresponding rates of weight loss. The thermolysis of lignin is related to its inherent structure and the various functional groups and the bond energies of them are an important factor. Figure 6 shows the bond energy of the different linkages in the β—O—4 structure to investigate the possible cracking in the thermolysis.[24] The mass loss from lignin occurred over a wide temperature range from 30 to 800°C. The thermal decomposition of PFL [Figure 5(a)] can be divided into three stages, different from two stages of CML. The initial stage between 30 and 141°C was mainly due to water release by evaporation and dehydration reactions and other low molecular weight volatiles of the lignin.[25] The second stage corresponded to 141–436°C was attributed to deformation of the weaker chemical bond in the β—O—4 structure. Most of the ether linkages were expected to be cleaved in this temperature range.[26] The lignin side chain oxidation including carbonylation/carboxylation of aliphatic hydroxyl group and side chain dehydrogenation occurred also at the second stage.[27] The final stage occurred after 436°C and the maximum mass loss presented at 534°C. It involved C—C bond cleavage and the cracking of the methoxy groups,[28] meanwhile, the decomposition of aromatic ring occurred in this stage.[29] Eventually, small amounts of char residues formed. In comparison with TGA curve of CML, it can be seen cleavage of ether linkages (especially β—O—4 structure) is obvious and the C—C bond cleavage and decomposition of aromatic ring occur later in TGA curve of PFL. This would ensure that hydroxyl is generated by cleavage of ether linkages and aromatic ring is not destroyed simultaneously at appropriate temperature in the thermolysis.

GPC and SEM

The molecular weights of acetylated lignin were investigated by GPC. The M_n of acetylated PFL and acetylated CML in THF was measured to be 2390 and 3228 with polydispersity index (M_W/M_n, PI) of 1.41 and 1.20, respectively. It was found that PFL separated from black liquor presented the lower M_n than that of CML and lignin from ball-milled bamboo.[12] The lignin with low molecular weight molecules is suitable for hydrogenated decomposition to form bio-oil because they are more reactive than those with high molecular weight. Moreover, in view

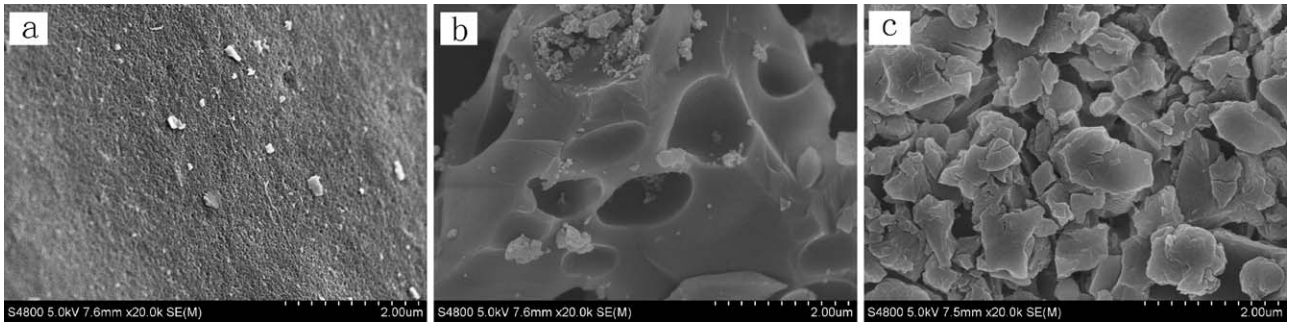

Figure 7. SEM micrographs of lignin: (a) crude lignin, (b) PFL, and (c) acetylated PFL.

of M_w/M_n, both kinds of lignin presented narrow molecular distribution, which indicated that lignin was formed with a relatively uniform lignin fragment size.

Figure 7 presents the SEM images of crude lignin, PFL and acetylated lignin, respectively. Three kinds of lignin have distinct difference in surface morphology. In Figure 7(a), the surface morphology of crude lignin was rough, showing some topographical features of moon. Some small holes can be detected under 50,000× magnification. In Figure 7(b,c), the lignin surface was basically smooth, and showed irregular fragment shapes with different sizes. Very few pores are presented in PFL surface and acetylated lignin hardly has any pores.

CONCLUSIONS

Crude lignin was separated from pulping black liquor by HCl-precipitation and purified by extraction with a mixture of dioxane and water. The content of lignin in black liquor was determined by UV spectroscopy through the calibration curve equation, and reached up to 34.8%. The yield could account for 74.4% of the total lignin composition. It showed abundant lignin could be obtained easily by simple process. The structural analysis revealed that recovered lignin preserved basic lignin structure, but had relatively lower amount of β—O—4 linkages, suggesting there was lignin degradation in pulping process. FTIR spectroscopy and ^{1}H NMR spectrometry revealed that lignin in black liquor is mainly composed by G and S units with high quantities of hydroxyl groups. XPS revealed the O/C ratio and high-resolution XPS scan analyzed the main existence type of C and O atoms. The cleavage of lignin linkage was related to the bond energy, therefore the weaker chemical bond in the β—O—4 structure cracked at first as the temperature increased. The molecular weights of acetylated lignin were studied through THF-eluted GPC showing that acetylated PFL had the lower M_n. The result showed lignin in black liquor had similar chemical structure with lignin directly obtained from lignocellulosic biomass. Moreover, partly-degradation and low molecular weights may be in favor of conversion of lignin to bio-oil. Therefore, lignin from black liquor has a significant potential and possibility as feedstock for bio-oil research even for industrial manufacture in the near future.

ACKNOWLEDGMENTS

The authors gratefully acknowledge financial support from the National Natural Science Foundation of China (No. 21203113) and Project of Development of Science and Technology of Shandong Province, China (No. 2013GZX20109).

REFERENCES

1. Zhang, W.; Chen, J.; Liu, R.; Wang, S.; Chen, L.; Li, K. *ACS Sustain. Chem. Eng.* **2014**, *2*, 683.
2. Laskar, D. D.; Tucker, M. P.; Chen, X.; Helms, G. L.; Yang, B. *Green Chem.* **2014**, *16*, 897.
3. Sedai, B.; Díaz-Urrutia, C.; Baker, R. T.; Wu, R.; Silks, L. P.; Hanson, S. K. *ACS Catal.* **2013**, *3*, 3111.
4. Sturgeon, M. R.; O'Brien, M. H.; Ciesielski, P. N.; Katahira, R.; Kruger, J. S.; Chmely, S. C.; Hamlin, J.; Lawrence, K.; Hunsinger, G. B.; Foust, T. D. *Green Chem.* **2014**, *16*, 824.
5. Pan, J.; Fu, J.; Deng, S.; Lu, X. *Energy Fuel* **2014**, *28*, 1380.
6. Sangha, A. K.; Davison, B. H.; Standaert, R. F.; Davis, M. F.; Smith, J. C.; Parks, J. M. *J. Phys. Chem. B* **2014**, *118*, 164.
7. Jin, W.; Tolba, R.; Wen, J.; Li, K.; Chen, A. *Electrochim. Acta* **2013**, *107*, 611.
8. Fu, K.; Yue, Q.; Gao, B.; Sun, Y.; Zhu, L. *Chem. Eng. J.* **2013**, *228*, 1074.
9. Velez, J.; Thies, M. C. *Bioresour. Technol.* **2013**, *148*, 586.
10. Lee, R. A.; Bédard, C.; Berberi, V.; Beauchet, R.; Lavoie, J.-M. *Bioresour. Technol.* **2013**, *144*, 658.
11. Guo, G.; Li, S.; Wang, L.; Ren, S.; Fang, G. *Bioresour. Technol.* **2013**, *135*, 738.
12. Wen, J.-L.; Xue, B.-L.; Xu, F.; Sun, R.-C.; Pinkert, A. *Ind. Crop. Prod.* **2013**, *42*, 332.
13. Wang, G.; Chen, H. *Sep. Purif. Technol.* **2013**, *105*, 98.
14. Hu, L.; Pan, H.; Zhou, Y.; Hse, C.-Y.; Liu, C.; Zhang, B.; Xu, B. *J. Wood Chem. Technol.* **2014**, *34*, 122.
15. Bu, L.; Tang, Y.; Gao, Y.; Jian, H.; Jiang, J. *Chem. Eng. J.* **2011**, *175*, 176.
16. Sun, Y.; Qiu, X.; Liu, Y. *Biomass Bioenerg.* **2013**, *55*, 198..
17. Manara, P.; Zabaniotou, A.; Vanderghem, C.; Richel, A. *Catal. Today* **2014**, *223*, 25.
18. Qian, Y.; Deng, Y.; Qiu, X.; Li, H.; Yang, D. *Green Chem.* **2014**, *16*, 2156.
19. Zhang, Y.; Wang, Q.; Fan, X.; Yuan, J. *J. Mol. Catal. B: Enzym.* **2014**, *101*, 133.
20. Wang, S.; Wang, Y.; Cai, Q.; Wang, X.; Jin, H.; Luo, Z. *Sep. Purif. Technol.* **2014**, *122*, 248.
21. Zhu, W.; Westman, G.; Theliander, H. *J. Wood Chem. Technol.* **2014**, *34*, 77.
22. Popescu, C.-M.; Tibirna, C.-M.; Vasile, C. *Appl. Surf. Sci.* **2009**, *256*, 1355.
23. Rasch, R.; Stricher, A.; Truss, R. W. *J. Appl. Polym. Sci.* **2014**, *131*, 39572.
24. Faravelli, T.; Frassoldati, A.; Migliavacca, G.; Ranzi, E. *Biomass Bioenerg.* **2010**, *34*, 290.
25. Luo, Z.; Wang, S.; Guo, X. *J. Anal. Appl. Pyrol.* **2012**, *95*, 112.
26. Wen, J. L.; Xue, B. L.; Sun, S. L.; Sun, R. C. *J. Chem. Technol. Biotechnol.* **2013**, *88*, 1663.
27. Ke, J.; Singh, D.; Yang, X.; Chen, S. *Biomass Bioenerg.* **2011**, *35*, 3617.
28. Yang, H.; Yan, R.; Chen, H.; Lee, D. H.; Zheng, C. *Fuel* **2007**, *86*, 1781.
29. Sun, Y.-C.; Xu, J.-K.; Xu, F.; Sun, R.-C.; Jones, G. L. *RSC Adv.* **2014**, *4*, 2743.
30. Sun, Y.-C.; Xu, J.-K.; Xu, F.; Sun, R.-C. *Ind. Crop. Prod.* **2013**, *47*, 277.
31. Del Río, J. C.; Rencoret, J.; Prinsen, P.; Martínez, A. N. T.; Ralph, J.; Gutiérrez, A. *J. Agr. Food Chem.* **2012**, *60*, 5922.
32. Nonaka, H.; Kobayashi, A.; Funaoka, M. *Bioresour. Technol.* **2013**, *140*, 431.